Biochimica et Biophysica Acta 1848 (2015) 1165–1174

Contents lists available at ScienceDirect

Biochimica et Biophysica Acta

journal homepage: www.elsevier.com/locate/bbamem

Secretory vesicle cholesterol: Correlating lipid domain organization and Ca^{2+} triggered fusion

Mark Mahadeo [a,1], Kendra L. Furber [b,1,2], Simon Lam [a,3], Jens R. Coorssen [c,d,*], Elmar J. Prenner [a,*]

[a] Department of Biological Sciences, University of Calgary, Calgary, Alberta, Canada
[b] Department of Physiology and Pharmacology, University of Calgary, Calgary, Alberta, Canada
[c] Molecular Physiology Department, School of Medicine, University of Western Sydney, Campbelltown, NSW, Australia
[d] Molecular Medicine Research Group, School of Medicine, University of Western Sydney, Campbelltown, NSW, Australia

ARTICLE INFO

Article history:
Received 19 September 2014
Received in revised form 2 January 2015
Accepted 7 February 2015
Available online 14 February 2015

Keywords:
Membrane fusion
Membrane domain
Cholesterol
Brewster angle microscopy

ABSTRACT

Membrane organization has received substantial research interest since the degree of ordering in membrane regions is relevant in many biological processes. Here we relate the impact of varying cholesterol concentrations on native secretory vesicle fusion and the lateral domain organization of membrane extracts from these vesicles. Membranes of isolated cortical secretory vesicles were either depleted of cholesterol, had cholesterol loaded to excess of native levels, or were depleted of cholesterol but subsequently reloaded to restore native cholesterol levels. Lipid analyses confirmed cholesterol was the only species significantly altered by these treatments. Treated vesicles were characterized for their ability to undergo fusion. Cholesterol depletion resulted in a decrease of Ca^{2+} sensitivity and the extent of fusion, while cholesterol loading had no effect on fusion parameters. Membrane extracts were characterized in terms of lipid packing by surface pressure–area isotherms whereas the lateral membrane organization was analyzed by Brewster angle microscopy. While no differences in the isotherms were observed, imaging revealed drastic differences in domain size, shape and frequency between the various conditions. Cholesterol depletion induced larger but fewer domains, suggesting that domain coalescence into larger structures may disrupt the native temporal–spatial organization of the fusion machinery and thus inhibit vesicle docking, priming, and fusion. In contrast, adding excess cholesterol, or rescuing with exogenous cholesterol after sterol depletion, resulted in more but smaller domains. Therefore, cholesterol is an important membrane organizer in the process of Ca^{2+} triggered vesicular fusion, which can be related to specific physical effects on native membrane substructure.

1. Introduction

Classically thought of as simply a barrier between intra- and extracellular compartments, biological membranes are in fact highly organized and actively participate in critical cellular functions. Depending on the lipid species present, distinct, spatially and temporally localized 'islands' may form as a result of the coexistence and immiscibility between liquid expanded (L_E) and liquid condensed (L_C) phases within leaflets of biological membranes. More or less rigid lipid regions have also been proposed to coexist with the largely liquid-crystalline native bilayer, constituting liquid ordered (L_o) and liquid disordered (L_d) lateral phases. With proteins present such lipid islands have also been referred to as microdomains [1,2]. The preferential interaction between cholesterol and phospholipids with long, saturated acyl chains, especially sphingolipids, is a primary driving force in the formation of lipid domains [3,4]. In cells, these microdomains have been characterized as highly dynamic, organized areas that serve as sites for specific protein–lipid and protein–protein interactions, thus facilitating or optimizing different membrane-associated functions [5,6]. As such, lipid composition and organization may regulate many cellular processes including signal transduction [7,8], and membrane trafficking [9,10]. A growing body of evidence supports the biological significance of more rigid domains, yet controversy still exists around the physical characteristics, or even the existence, of these domains in vivo [1,2,11]. This is largely due to the technical limitations of studying lipid and protein dynamics in native membranes [6]. There has been a surge in the study of

Abbreviations: BAM, Brewster angle microscopy; CV, cortical vesicles; mβcd, methyl-β-cyclodextrin; hpβcd, hydroxypropyl-β-cyclodextrin; Chol, cholesterol; HPTLC, high performance thin layer chromatography; L_E, liquid expanded; L_C, liquid condensed; L_o, liquid ordered; L_d, liquid disordered; FFM, fundamental fusion mechanism; PFM, physiological fusion machines

* Corresponding authors.
E-mail addresses: J.Coorssen@uws.edu.au (J.R. Coorssen), eprenner@ucalgary.ca (E.J. Prenner).

[1] Both authors contributed equally to the work.
[2] Current address: College of Pharmacy and Nutrition, University of Saskatchewan, Saskatoon, Saskatchewan, Canada.
[3] Current address: Department of Pediatrics, University of Calgary, Calgary, Alberta, Canada.

http://dx.doi.org/10.1016/j.bbamem.2015.02.005
0005-2736/

cholesterol and lipid domains in cellular function, in particular with regard to regulated secretion [9,10] which is a highly conserved process for the release of neurotransmitters, hormones and other bioactive molecules. Since the original observations concerning cortical vesicle (CV) fusion [12–14], alterations in membrane cholesterol have been shown to affect exocytotic events in nerve terminals [15–20] neuroendocrine cells [21–23], β cells [24], and endothelial cells [25].

Cholesterol is highly enriched in eukaryote secretory vesicles [26] and the merger of biological membranes is dependent on the presence of cholesterol at the fusion site [12,13,27] Isolated CV from sea urchin oocytes are a stage-specific model to investigate mechanisms of Ca^{2+} regulated membrane fusion separate from other membrane trafficking events [9,28]. The advantage of the CV model is that isolated vesicles remain fusion competent in vitro. CV have comparable Ca^{2+} sensitivity, fusion kinetics, and molecular composition to other secretory vesicles [26,29,30] and CV–CV and CV–plasma membrane fusion, proceed through a common underlying mechanism [63]. Studying CV–CV fusion enables separation of the docking and membrane merger stages of exocytosis as well as direct characterization of CV membrane; ample material is available to carry out several types of analyses in parallel. Together, these unique properties enable direct assessment and correlation of fusion parameters and select membrane properties to identify critical components of the native fusion machinery [14,27,31–35].

Due to the complexity of the secretory pathway, definitive roles for cholesterol in the molecular mechanisms underlying specific stages of exocytosis (i.e. vesicle trafficking, docking, priming, Ca^{2+}-sensing, and membrane fusion) remain less well defined. However, as studies with CV enable the assessment of docking and Ca^{2+}-triggered membrane fusion in isolation from other stages of the secretory pathway, both a prefusion (i.e. likely defining the docking and fusion site) and a direct role for cholesterol in the fusion mechanism itself have been clearly established (reviewed in [9]); the latter has been confirmed by the more recent assessment of fusion pore properties [21,22]. Depletion of CV cholesterol results in a concentration-dependent decrease in the rate, Ca^{2+} sensitivity and overall extent of vesicle fusion, which can be recovered by supplementation with exogenous cholesterol [12,13,27]. While the ability of vesicles to fuse correlates with a critical negative curvature contributed by cholesterol [13], the efficiency of the triggering mechanism (rate and Ca^{2+} sensitivity) appears to be dependent on the integrity of membrane microdomains. The depletion of either cholesterol [12,27] or sphingomyelin [14], which is known to disrupt microdomains [36–38] result in a decrease in Ca^{2+}-sensitivity. Cholesterol depletion also reduced the fraction of isolated cholesterol-enriched membranes, which are considered to reflect overall native microdomain composition [39]. These findings have largely been confirmed in a range of other secretory vesicles and cell types, including synaptic vesicles [15,31] and Weibel–Palade bodies [25]; as might be expected, the data tend to be somewhat more complicated in intact cells and tissues, attesting to the broader role of such microdomains in the localized regulation of a range of native functions [20,21]. However, to date, the functional domains have not been visualized directly in secretory vesicles.

Advances in microscopy techniques, such as single-particle tracking [40–44] and super-resolution imaging [45–47], have started to clarify questions surrounding domain structure and dynamics. As these imaging techniques necessitate the addition of exogenous lipid dyes, over-expression of fluorescently tagged proteins or the addition of antibodies to the cell surface, there may be additional influences on the native system. Here, we have used established methods to manipulate the CV membrane cholesterol content, analyze the architecture of microdomains, and correlate this with quantitative assessments of changes in fusion parameters and membrane composition [12–14, 27,34]. Lipid organization was investigated in monolayers from CV membrane extracts by recording area isotherms at the air–water interface; this enabled the investigation of lipid packing as described by the average area per molecule [48] as well as direct visualization of domain structures using Brewster angle microscopy (BAM) [49,50].

Working with monolayers at the air–water interface enables precise control of lipid composition and this approach has been used extensively to study lipid packing, the impact of ligands on membrane structure and the lateral domain organization in membranes [51–54]. Monolayer membrane properties, including lateral pressures of 30 to 35 mN/m, were found to be equivalent to bilayer properties [55]. As well, Langmuir monolayer experiments can be coupled with various imaging techniques to assess lateral film organization [56]. BAM is particularly well suited as it enables label free imaging of the lateral organization of the membrane in real time [49]. In contrast to fluorescent protein and lipid probes often used to visualize microdomains [57]. The development of BAM techniques has significantly advanced our understanding of the role of specific lipids in domain formation in biomimetic monolayers [58]. This approach has also enabled the characterization of membrane protein clusters [53] and the identification of an annular lipid, an unsaturated cardiolipin, which was shown to determine the actual formation and localization of oligomers of the hydrophobic membrane protein, EmrE [54]; biochemical data of the oligomerization are consistent with the biophysical findings [59,60]. Domain formation was also observed for other membrane proteins [61,62] and comparable structures have also been proposed for bacterial systems [63,64].

Here we report the impact of i) manipulating secretory vesicle cholesterol content and correlate biophysical observations on domain formation with biochemical data on membranes composition; and ii) domain parameters on function, especially the extent and Ca^{2+} sensitivity of triggered membrane fusion, in order to better understand the role of membrane architecture in the late steps of regulated exocytosis and triggered membrane fusion.

2. Methods

2.1. Cortical vesicle preparation

Strongylocentrotus purpuratus were obtained Westwind SeaLab Supplies (Victoria, B.C.) and kept in artificial sea water (Instant Ocean) at 7 °C until unfertilized oocytes were collected. Cortical vesicles were isolated as previously described [12–14,65], and suspended in baseline intracellular media (BIM; pH 6.7) supplemented with 2.5 mM adenosine-5′-triphosphate, 2 mM dithiothreitol and protease inhibitors for all subsequent treatments and functional analyses [66]. Stock solutions of 100 mM methyl-β-cyclodextrin (mβcd; Sigma, St. Louis, MO) and cholesterol (Avanti Polar Lipids, Alabaster, AL)-loaded hydroxyl-propyl-β-cyclodextrin (hpβcd; Sigma, St. Louis, MO) were prepared in BIM, as previously described [12], and added to CV suspensions (OD ~ 1.0) at the final concentration of 2 mM for 30 min at 25 °C. Cholesterol depletion was achieved by treatment of the CV samples with mβcd, while control samples were left untreated. Subsequent treatment of a subset of both the cholesterol depleted and control treatments with cholesterol-loaded hpβcd yielded cholesterol rescued and excess cholesterol loaded conditions, respectively. Following treatments, CV were washed by centrifugation and suspension in fresh BIM, and then aliquoted for lipid extraction (OD ~ 1.0) or functional analyses (OD ~ 0.30).

Fusion was assessed at room temperature using a standard light-scattering assay [12,65] 3–4 replicates per sample. Ca^{2+} activity curves were normalized to controls and fit with a cumulative log function using TableCurve 2D v5.01 (SYSTAT, Richmond, CA) to assess the extent and EC_{50} [67].

2.2. Molecular analyses

CV lipids were extracted using a modified Bligh and Dyer method [12,68]. Extracts were dried and stored (−80 °C) under inert gas (N_2

or Ar) until further analyses. Lipid composition was determined by high performance thin-layer chromatography (HPTLC) according to [26,27], with slight modification. Dried CV membrane lipid extracts and purified lipid standards (Avanti Polar Lipids, Alabaster, AL) were solubilized in $CHCl_3$:CH_3OH (2:1; v/v) and loaded onto activated silica gel 60 TLC plates (EMD Chemicals, Gibbstown, NJ) with the Linomat IV (CAMAG, Wilmington, NC). Lipids were resolved by automated, sequential separation steps in the AMD 2 multi-development unit (CAMAG, Wilmington, NC), optimized for the separation of either i) neutral lipids—CH_2Cl_2/ethyl acetate/acetone (80:16:4; v/v/v) to 45 mm, and then hexane/ethyl acetate (92:8; v/v) to 63 mm, (95:5; v/v) to 80 mm and (98:2; v/v) to 90 mm; or ii) phospholipids—CH_2Cl_2/ethyl acetate/acetone (80:16:4; v/v/v) to 90 mm, and then $CHCl_3$/methanol/ethanol/ethyl acetate/acetone/iospropanol/water/acetic acid (30:28:16:6:6:6:6:2; v/v/v/v/v/v/v/v) to 90 mm. Plates were charred with $CuSO_4$ and the resulting fluorophore detected with 540/30 excitation and 590/30 emission filters in the ProXpress Imager (PerkinElmar, Boston, MA). For quantification, the integrated fluorescent signal from CV membrane lipids was compared to a parallel dilution series of standards on the same plate using ImageQuant v5.2 (GE HealthCare, Piscataway, NJ); $n = 5–6$ for cholesterol and $n = 2–5$ for other lipids. Protein content was determined using the EZQ Protein Quantitation Kit (Life Technologies Inc., Burlington, ON), according to manufacturer's instructions.

2.3. Surface pressure–area isotherms

Lipid packing parameters were measured by recording surface pressure–area isotherms [51]. Aliquots of the same lipid extracts as used for the quantitative molecular analyses were solubilized in $CHCl_3$:CH_3OH (2:1, v/v) at 2 mg/mL and 40 uL of sample was deposited on a Langmuir trough (Nima technology, Coventry, England) in a drop-wise manner onto a double distilled H_2O sub-phase at room temperature. The monolayer was left for 10 min in order for the solvent to evaporate. The barriers were set to compress the lipids at 100 cm^2/min with the minimal area set at 20 $Å^2$/molecule and the surface pressure was measured by a pressure sensor (Nima Technology, Coventry, England). Data were recorded using NIMA v5.16 (Nima Technology, Coventry, England) which requires the designation of a specific molecular weight; due to the complexity of this biological sample, 809 g/mol was used to approximate the most common chain lengths for the lipids and fatty acids present in the species [26,69]. For each sample, 3–9 replicate area–pressure isotherms were measured.

2.4. Brewster angle microscopy imaging

To visualize lipid organization, the Langmuir trough was adapted for a BAM microscope (EP3 BAM, Nanofilm Technologie GmbH, Göttingen, Germany). A 20× objective lens was used to give about 1 μm lateral resolution and the light source was a 50 mW Neodymium: Yttrium–Aluminium–Garnet (NdYAG) laser set at 532 nm. As the laser is reflected off the surface of the monofilm at the air–water interface, structures protruding from the film along the z-axis will appear brighter. Thus increased brightness upon compression suggests a film reorganization resulting in relative increase in film thickness. The sample handling was identical to the surface pressure–area isotherm monolayer films except that during compression the barriers were stopped at several intervals to capture images. The pressures at which images were obtained were based on the results from the surface pressure–area isotherms (see results section). Images were recorded using EP^3 view software (Accurion, Göttingen, Germany). For each condition, 3 representative images were selected at the indicated surface pressures and analyzed with Image J software (NIH, Bethesda Maryland USA).

3. Results

3.1. Coupled quantitative functional and molecular analyses

Fusion of control CV yielded a characteristic sigmoidal Ca^{2+} activity curve with an EC_{50} of 35.0 ± 2.3 μM $[Ca^{2+}]_{free}$ (Fig. 1 A, B), in agreement with previous reports on CV–CV and CV–plasma membrane fusion [12–14,27,34,65,67]. To determine the effect of cholesterol on Ca^{2+} triggered membrane fusion, cyclodextrins were used to remove or deliver cholesterol [12–14,20,21]. Treatment of free-floating CV with 2 mM mβcd for 30 min at 25 °C (ie. cholesterol depleted condition) reduced the number of fusion competent CV to 61.8 ± 9.9% ($p = 0.008$). The Ca^{2+} sensitivity of triggering was also inhibited to an EC_{50} of 69.7 ± 5.0 μM $[Ca^{2+}]_{free}$ ($p < 0.001$). Delivery of exogenous cholesterol to cholesterol-depleted CV (i.e. cholesterol rescued condition) resulted in full recovery of both the extent (95.9 ± 9.9%) and Ca^{2+} sensitivity (44.7 ± 4.0 μM $[Ca^{2+}]_{free}$) of fusion. Delivery of exogenous cholesterol to control CV (i.e. cholesterol loaded condition) had no significant effect on fusion (Fig. 1A, B).

Lipid extractions were carried out in parallel with fusion assays and the resulting isolates were subjected to further molecular and biophysical analyses. To confirm selective cholesterol removal or delivery by the cyclodextrins, CV lipid composition was analyzed by HPTLC (Table 1). Native CV membranes were enriched in cholesterol at 16.4 ± 0.4 mol% or a cholesterol: total lipid ratio of 0.20 ± 0.01 (Fig. 1C). Treatment of control CV with 2 mM mβcd (ie. cholesterol depleted) decreased CV cholesterol to 12.2 ± 0.4 mol% (Table 1; $p < 0.001$). Treatment of cholesterol-depleted or control CV (i.e. cholesterol rescued and cholesterol loaded, respectively) with 2 mM cholesterol-loaded hpβcd increased cholesterol to 22.4 ± 0.7 mol% and 22.6 ± 0.4 mol% (Table 1), respectively (cholesterol: lipid ratio of 0.29 ± 0.01 in both cases). A decrease in cholesterol correlated directly with a decrease in the Ca^{2+} sensitivity and extent of fusion, and this was rescued by the incorporation of exogenous cholesterol. In contrast, an increase in cholesterol beyond native levels did not have any effect on fusion extent or Ca^{2+} sensitivity (Fig. 1).

3.2. Quantitative structural analyses

CV lipid extractions underwent further biophysical and domain characterization using the Wilhelmy plate method [70]. Such monolayers have proven to be effective models for a variety of mammalian and bacterial membranes [71]. The surface pressure–area isotherms of the CV monolayers (Fig. 2) all exhibited a comparable shape that was largely retained regardless of the different treatment conditions of the original CV. While the isotherms initially exhibited a consistent gentle slope under all conditions, which could be interpreted as L_E phase, BAM images at very low pressures of 5 mN/m already showed well developed L_C domains (Fig. 3) thus demonstrating phase coexistence even early in the compression paradigm. Indeed, short range interactions between molecules can induce phase co-existence [72] in localized patches of the monolayer. All of the isotherms begin to increase in pressure between 87 and 90 $Å^2$/molecule, denoting transition from the so called gas phase, in which the lipids in the monolayer have very little order and few constraints on molecular motion, into coexisting L_E–L_C phases. Whereas the former has few constraints on the molecular motion of the acyl tails, the latter is characterized by more intermolecular interactions and increased rigidity [73]. The slight plateau region observed in the isotherms between the pressures of ~18–21 mN/m could be interpreted as an indicator of phase co-existence; however, as these already contained both L_E–L_C, other changes in the film must be considered. Interestingly, this plateau is observed in a lateral pressure range in which monofilms of membrane proteins have been reported to denature [53,74] and it is quite feasible that some hydrophobic proteins were extracted into these samples. Indeed, we have seen protein domains in extracts of yeast membranes, which are an equally complex

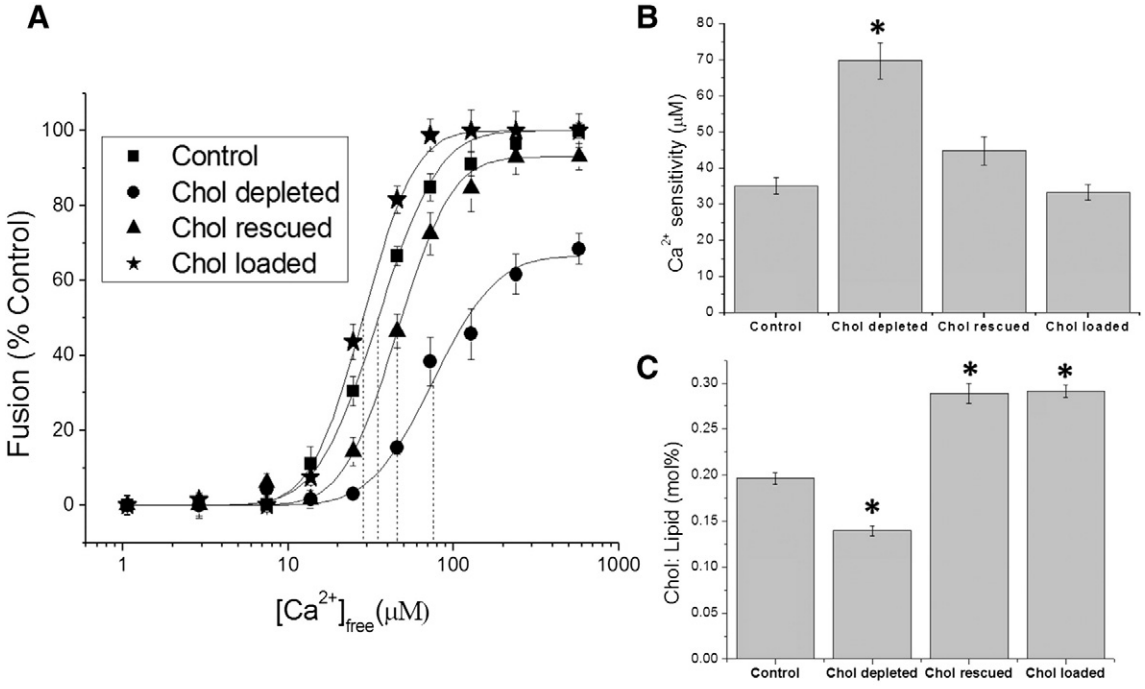

Fig. 1. The effect of cholesterol on Ca^{2+} triggered membrane fusion. (A) Ca^{2+} activity curves for untreated (control), mβcd treated (Chol depleted), and cholesterol loaded hpβcd (Chol loaded) cortical vesicles (CV), as well as CV receiving successive treatments with mβcd and cholesterol loaded hpβcd (Chol rescued). Changes in Ca^{2+} activity (EC_{50} for $[Ca^{2+}]_{free}$) (B); and lipid: cholesterol ratios (C) with respect to the treatments in (A). Data reported as mean ± SEM (n = 4); *p < 0.01 compared to control.

biological matrix (Mahadeo et al, unpublished observations). Above this plateau region the monolayer exhibits an increasing number of rigid domains, representing L_C phase before monolayer collapse is observed between ~38–41 mN/m. At this point the monolayer can no longer be compressed further and lipids begin to either submerge into the subphase, or stack on top of one another to form multilayers.

To analyze domain characteristics, a second set of isotherms was recorded during which the monolayer compression was stopped at 5.5 ± 0.1 mN/m, 15.6 ± 0.3 mN/m, 24.6 ± 0.4 mN/m and 32.4 ± 0.4 mN/m (Fig. 3). These pressures were selected due to the presence of the inflection point at ~ 20 mN/m in the isotherms (Fig. 2) with analysis of images occurring for two points above and two points below this pressure to fully capture the behavior of the film. As well, the last point selected (~30 mN/m) correlates to physiological pressures found in bilayers [55]. The BAM images for the control CV extract showed a low frequency of large domains at both 5.1 mN/m and 15.8 mN/m. In contrast, at 22.1 mN/m a much higher frequency of smaller domains was observed. Upon further compression to 33.9 mN/m the frequency of domains was relatively constant, but these increased in both size and reflective intensity. In the images of the cholesterol depleted samples, a similar trend was observed at both 5.7 mN/m and 14.5 mN/m, with predominantly large domains at a low frequency. Again, upon compression to 24.6 mN/m and 32.9 mN/m, the domains increased in frequency and brightness, but decreased in size (especially at 32.9 mN/m, at which there occurred a quite marked decrease in size). Extracts of cholesterol rescued CV yielded smaller domains that formed at a much higher frequency at both 6.3 mN/m and 15.7 mN/m relative to the control. We have recently reported similar changes based on the formation of defined clusters of the bacterial membrane protein EmrE [53,54]. As the films analyzed here are extracts of complex native membranes, the presence of some hydrophobic membrane proteins is to be expected. Much smaller, brighter domains were observed at 25.0 mN/m, while at 30.6 mN/m the number of domains sharply increased, but these remained relatively constant in size. Finally, for the extracts from CV that had been loaded with excess cholesterol, a large number of small domains were initially observed at 5.8 mN/m. While the number of domains steadily increased during compression, the size of domains decreased between 5.8 mN/m and 16.7 mN/m, and then

Table 1
The lipid composition of membrane extracts from control CV as well as CV that had been treated with either mβcd (Chol depleted) or cholesterol loaded hpβcd (Chol loaded), or first by mβcd followed by cholesterol loaded hpβcd (Chol rescued). Data reported in mol% as mean ± SEM (n = 5–6 for cholesterol and 2–5 for other lipids).

Lipid	Control	Chol depleted	Chol rescued	Chol loaded
Cholesterol	16.4 ± 0.4	12.2 ± 0.4*	22.4 ± 0.7*	22.6 ± 0.4*
Triacylglycerol	29.6 ± 2.0	30.6 ± 1.1	24.7 ± 0.9	24.9 ± 1.6
Diacylphosphatidylcholine	17.0 ± 0.8	15.1 ± 1.8	19.3 ± 1.9	20.1 ± 1.7
Fatty acids	5.8 ± 1.4	7.9 ± 1.9	7.8 ± 2.1	7.5 ± 0.9
Diacylphosphatidylinositol	6.6 ± 1.6	7.3 ± 2.2	6.5 ± 2.0	6.3 ± 1.6
Diacylphosphatidylethanolamine	4.0 ± 1.0	6.4 ± 0.8	4.8 ± 0.6	3.5 ± 0.9
Lysophosphatidylethanolamine	4.0 ± 1.6	3.3 ± 0.5	3.4 ± 1.0	3.5 ± 0.9
Monoacylglycerol	4.3 ± 1.1	2.8 ± 0.8	3.1 ± 0.2	3.1 ± 0.5
Diacylphosphatidylserine	3.7 ± 1.0	3.7 ± 1.0	3.1 ± 1.0	3.1 ± 1.3
Diacylphosphatidylglycerol	1.7 ± 0.4	1.9 ± 0.1	2.9 ± 0.7	2.3 ± 0.3
Diacylglycerol	1.9 ± 0.5	2.0 ± 0.3	2.1 ± 0.4	2.1 ± 0.7
Cholesterol esters	0.6 ± 0.0	0.6 ± 0.1	0.5 ± 0.1	0.5 ± 0.1

* p < 0.001 compared to control.

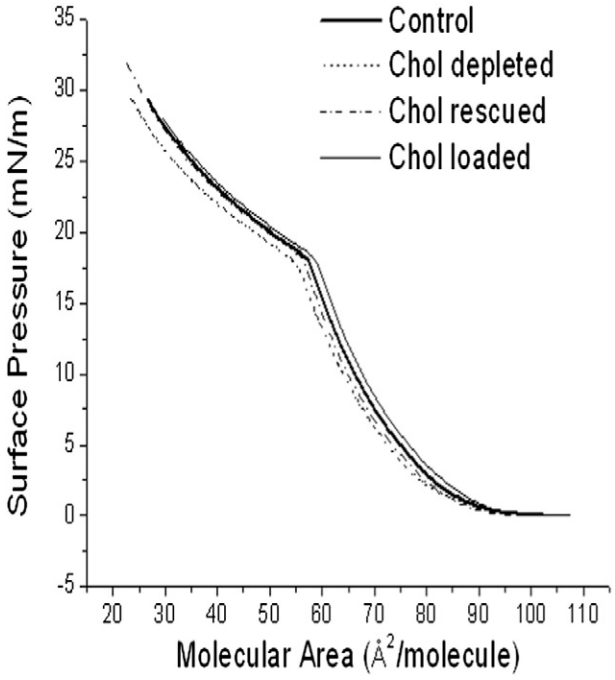

Fig. 2. Surface pressure–area isotherms of membrane extracts of CV treated with mβcd (Chol depleted), cholesterol loaded hpβcd (Chol loaded), and both (Chol rescued), as well as untreated control (n = 4).

remained constant as the monolayer was compressed to higher pressures. Overall, the number of domains was found to increase with an increase in pressure (Fig. 4A) while the size of the domains decreased (Fig. 4B). Interestingly, the total domain area remained relatively constant except at the pressure extremes (Fig. 4C). The domains had a circular shape which also remained relatively constant over a large pressure range (Fig. 4D). Cholesterol depletion resulted in a decrease in the number of domains at 24.6 ± 0.4 mN/m ($p = 0.008$) and 32.4 ± 0.4 mN/m ($p = 0.009$). This was mirrored by an increase in domain size at 5.5 ± 0.1 mN/m ($p = 0.041$) and 24.6 ± 0.4 mN/m ($p = 0.005$). Extracts of cholesterol rescued CV exhibited not only recovery of the number of domains at 24.6 ± 0.4 mN/m, but also an increase in the number at 5.5 ± 0.1 mN/m ($p = 0.039$) and 32.4 ± 0.4 mN/m ($p = 0.004$). Extracts of cholesterol loaded CV exhibited an increase in the number of domains at 5.5 ± 0.1 mN/m ($p = 0.049$), 15.6. ± 0.3 mN/m (0.004), and 32.4 ± 0.4 mN/m ($p = 0.002$). Similarly, extracts of cholesterol rescued CV displayed reduced domain size comparable to control values at 5.5 ± 0.1 mN/m and 24.6 ± 0.4 mN/m, and cholesterol-loading in control CV decreased the domain size at 5.5 ± 0.1 mN/m ($p = 0.042$) and 15.6 ± 0.3 mN/m ($p < 0.001$). Thus, in summary, a decrease in cholesterol correlated with a decrease in domain frequency and an increase in domain size while an increase in cholesterol correlated to an increase in domain frequency and decrease in domain size.

4. Discussion

Lipids and proteins are the major building blocks of mammalian membranes, define their lateral organization and thus localized functions. Accordingly, the concept of membrane domains has gained significant interest in mammalian [1,5] and bacterial membranes [63,64] as part of ongoing efforts to better understand the relationship(s) between membrane structure and physiological functions. This has become of particular interest with regard to regulated membrane fusion, which is among the most fundamental of cellular processes. Here we correlate, seemingly for the first time, detailed quantitative biochemical and functional data on membrane fusion with biophysical data on the lateral domain organization of the well-established CV model system that has yielded critical information concerning many fundamental characteristics of regulated exocytosis [9,28,31,33,35,67,75,76].

The role of cholesterol in heterotypic (vesicle–plasma membrane) and homotypic (vesicle–vesicle) fusion has been rigorously analyzed using the CV model system. Well established sigmoidal Ca^{2+} activity curves for CV fusion (Fig. 1) reflect both the ability of vesicles to fuse (extent) and the efficiency of the reaction (Ca^{2+} sensitivity) [12–14,27,31,32,34,65,67]. Cholesterol depletion results in both a decrease in the extent and Ca^{2+} sensitivity of fusion without altering the underlying shape of the Ca^{2+} activity curve. This indicates that loss of membrane cholesterol does not alter the underlying molecular mechanisms per se but rather is a component of the mechanism(s) [9,12,27,65,67]. Thus, alterations in fusion parameters following cholesterol depletion reflect both a reduction in the numbers of viable fusion sites or complexes (i.e. the fundamental fusion mechanism; FFM) as well as physiological fusion machines (PFM) that include components defining reaction efficiency (e.g. Ca^{2+} sensitivity) [9,27,35]. Delivery of exogenous cholesterol rescues both the extent and Ca^{2+} sensitivity of fusion; previous studies have established rescue of fusion kinetics as well, but this was not assessed in the current study [12,13,27]. The FFM is dependent on the negative curvature contribution of cholesterol and other lipids (i.e. at the fusion site); after cholesterol depletion, supplementation with other lipids of specific negative curvature recovers the ability of CV to fuse but not the efficiency of the reaction. [12,13,27]. This indicates a second role for cholesterol in fusion efficiency (i.e. it is also a critical component of the PFM). While not measured in the current study, a small amount of sphingomyelin (<0.15 mol%) is present in the CV membrane [26] and acts, in conjunction with cholesterol, to regulate fusion efficiency [14]. Depletion of cholesterol or sphingomyelin results in a decrease in Ca^{2+} sensitivity [12,14] and a loss of the cholesterol-enriched CV membrane fraction generally considered representative of microdomains [39]. On the other hand, sequestration of cholesterol or sphingomyelin within the membrane, using selective binding reagents, does not affect Ca^{2+} sensitivity [12,14] or disrupt cholesterol-enriched membrane isolates [39]. Thus, the integrity of microdomains appears to ensure the collective functioning of the PFM for optimized efficiency, presumably by organizing critical components involved in vesicle docking, priming, Ca^{2+} sensing and triggering. Interestingly, an increase in cholesterol content above native levels does not result in an enhancement of fusion suggesting that the lipid composition of the CV membrane is already optimized for efficient fusion, and thus that there is only a fixed amount of available PFM components per vesicle [12–14,26–28,31,34,66,67,76].

Biophysical analyses of the packing and lateral organization of the CV extracts involved assessment of monolayer isotherms coupled with Brewster angle microscopy. Comparable studies of native membrane extracts have largely focused on lung surfactant, yielding detailed characterization [77–79], as well as on myelin membrane [80]. Moreover, lateral domains have been identified in both red blood cell [81] and *Escherichia coli* extracts [54].

Here we assessed relative trends in the surface pressure–area isotherms (Fig. 2); due to the complex composition of CV extracts, only an approximate 'general' molecular weight could be entered into the Nima program used to record the isotherms. Nonetheless, no significant shifts of the isotherms were observed regardless of the treatment used (i.e. cholesterol depletion, re-loading, or excess loading); isotherms for the different treatments as well as the control extracts shared a common profile. This is perhaps not surprising as marked alterations in membrane cholesterol have no effect on capacitance [21]. The relatively gentle slopes at the onset of these isotherms, and also past the plateau region in the higher pressure regime, indicate moderately tight lipid packing, presumably due to the presence of unsaturated acyl chains that prefer fluidity and reduced packing, consistent with what

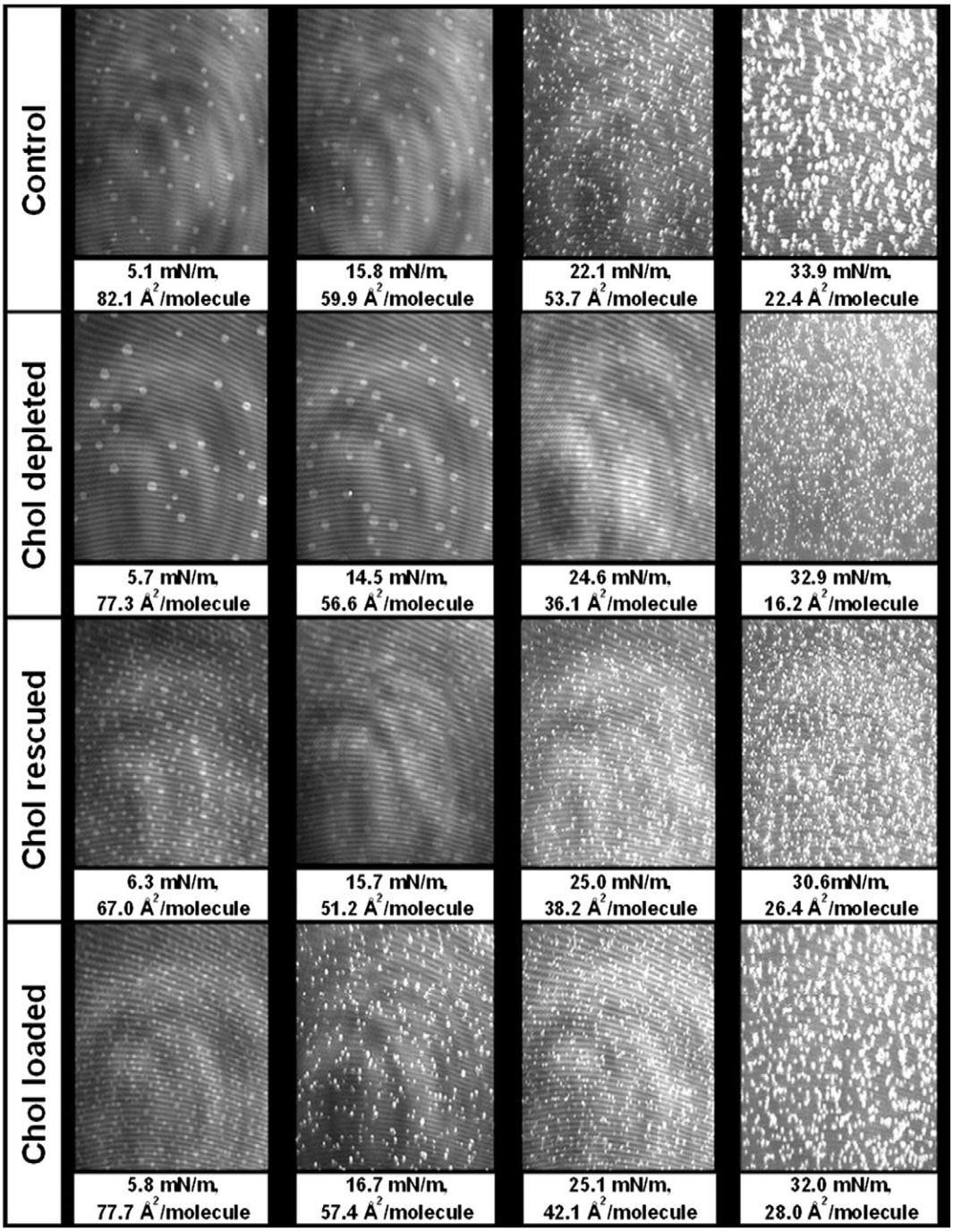

Fig. 3. Representative Brewster angle microscopy (BAM) images of lateral organization in CV membrane lipid extracts. Domain analysis was conducted for extracts of CV treated with mβcd (Chol depleted), cholesterol loaded hpβcd (Chol loaded), and both (Chol rescued), as well as untreated control. Each image represents 271 × 219 μm^2 of membrane.

is known of the CV membrane lipid profile (which is also comparable to that of other secretory vesicles) [26]. Consistent with previous work, the only lipid species that differed significantly between treatments was cholesterol (Table 1). While numerous studies have shown that cholesterol has a condensing effect [82–89], these generally involved simple binary or tertiary systems composed of synthetic lipids with acyl tails of consistent length. Therefore in these cases, changes in the proportions of cholesterol would have a very substantial effect on the properties of the monolayer. Notably, however, even in such simple lipid model systems, it is known that cholesterol can have quite different effects, including the promotion of high curvature structures, depending on the nature of the neighboring lipids [90]; this would certainly be the case in microdomains and at the interface of domains and 'bulk' membrane. Furthermore, as can be observed from the bright domains in the BAM images (Fig. 3), some hydrophobic proteins and/or peptides were present in the CV extracts. While the amount of protein is under the limit of detection for protein assays, it may still be enough to exert influence on the monolayer and be detectable in the BAM images, particularly under the higher pressures used. We have previously demonstrated that similar bright and protruding domains are due to the presence of hydrophobic membrane proteins [53] but are also strongly influenced by the presence of particular lipids [54]. Thus, considering the presence of many different lipids as well as hydrophobic proteins and peptides, and the relatively small difference in cholesterol content between treatments (4–6%), this likely explains why the overall macro-level phase behavior of the monofilm appeared unchanged.

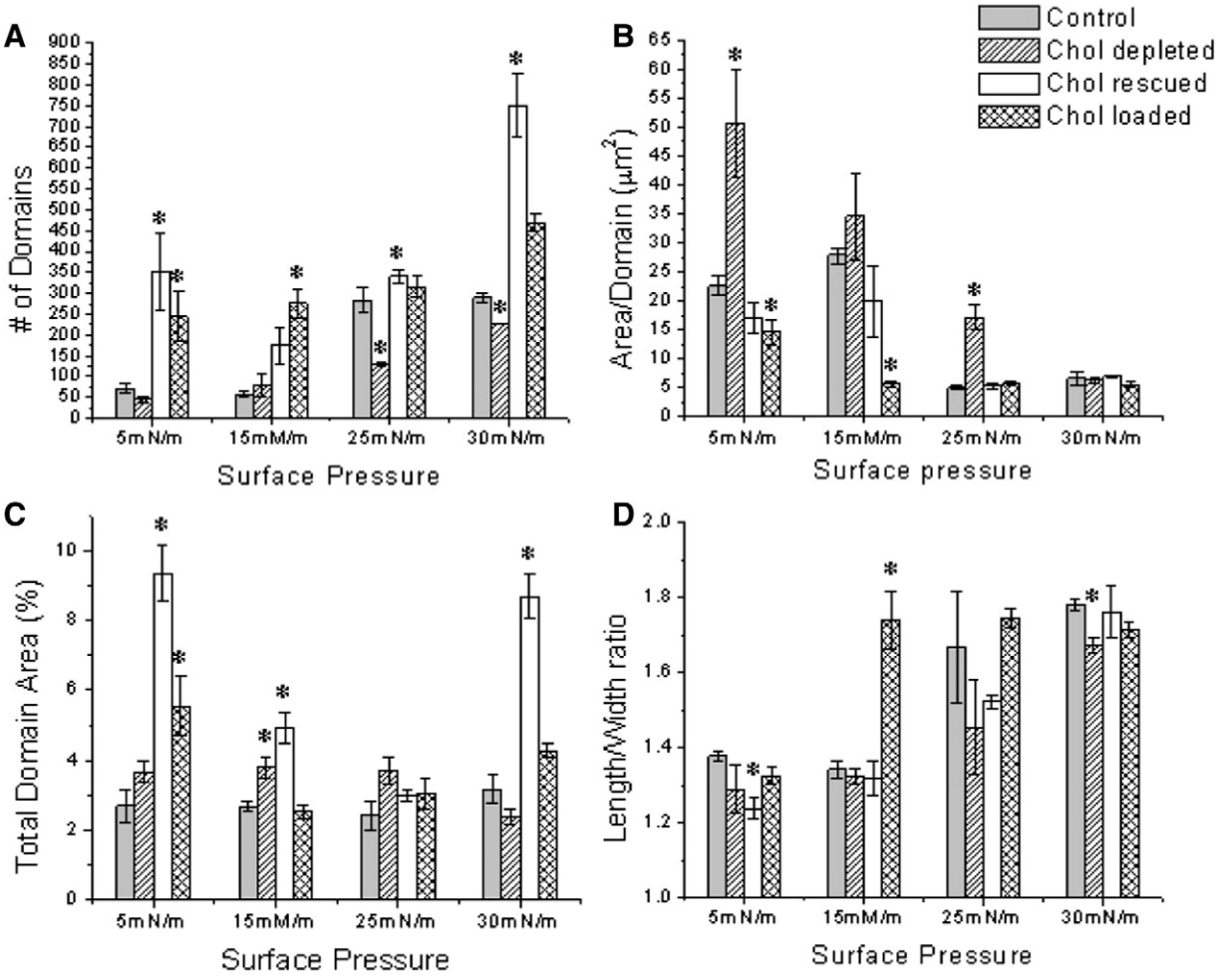

Fig. 4. Summary of the effects on domains of the treatments used to manipulate CV membrane cholesterol content: domain parameters analyzed included (A) frequency, (B) size, (C) total area, and (D) shape. Data reported as mean ± SEM (n = 3); *p < 0.05 compared to control.

Notably, despite no marked change in the packing behavior of the CV extract monofilm, there was a very striking difference in the lateral organization and domain formation upon alteration of cholesterol levels in the membrane (Fig. 3). Domains were present throughout the compression paradigm, with the most pronounced differences in phase separation being observed at low levels of compression. This has also been observed in extracts of myelin membranes [80]. The presence of these immiscible domains at low pressures serves to illustrate that even with little external force acting on the membrane, the lipids segregate and form discrete coexisting phases as a result of line tension generated by the hydrophobic mismatch between the L_C domains within the L_E bulk monofilm [91–93]. Thus, cholesterol concentration plays a large role with regards to domain size, shape and frequency (Fig. 3 and 4).

The frequency and size of domains in the different conditions display a general trend of increasing domain frequency and decreasing domain size upon monolayer compression (Fig. 4A and B). Relative to control extracts, cholesterol depleted extracts had the fewest domains present at most pressure values (i.e. significantly less than the control at pressures above 20 mN/m), while cholesterol loading resulted in significantly higher domain frequency and decreased size at most pressures. This condensation of domain size, even at low pressures, is likely due to the presence of cholesterol reducing line tension between the phases [94]. Thus, in cholesterol loaded samples, domains were significantly smaller at 15 mN/m, while remaining relatively constant in size during the entire compression. Smaller domains were not observed in the cholesterol rescued or control extracts below pressures of ~25 mN/m, and not until pressures in excess of 30 mN/m for the cholesterol depleted extracts.

In both the control and cholesterol depleted samples, large domains were observed with an infrequent abundance at low levels of compression (Fig. 4A). The proportions of cholesterol in these samples are 16.4 ± 0.4 mol% and 12.2 ± 0.4 mol%, ($p < 0.001$) respectively. In contrast, the cholesterol loaded and cholesterol rescued samples (proportions of cholesterol were 22.6 ± 0.4 mol% and 22.4 ± 0.7 mol%, respectively) consisted of small domains that formed with a high frequency. This phenomena has also been observed in bovine lung extract surfactant in which an addition of 4 mol% cholesterol lead to a decrease in the size of the liquid condensed phase domains [78]. In model membranes, the rigidifying effect of cholesterol has a strong dependence on both the cholesterol concentration and the overall lipid composition [86]; strong associations between cholesterol and both sphingolipids [3,4] and saturated lipid tails [95] result in the formation of very rigid L_o phases. However, the presence of unsaturation weakens the rigidifying effect and promotes the segregation of cholesterol from the L_d phase into domains of high cholesterol concentration. Therefore, it is perhaps not surprising that both treatments that added cholesterol to the CV membrane resulted in a condensation of domains. At a certain point during compression of the monolayer, the domains in both the control and cholesterol depleted CV extracts a change in size

from large to small, suggesting fission of the domains; a likely reason for this could be the increase in the localized level of cholesterol upon monolayer compression. For example, samples with less cholesterol required more compression to exhibit smaller domains (Fig. 3). In the control samples, these domains were not observed until pressures above 20 mN/m (Fig. 3). Similar domains were observed to form in the cholesterol depleted sample only after much higher levels of compression whereas in both extracts from cholesterol loaded CV, these domains seem to be present from the onset. As the monolayer was compressed, intermolecular lipid–lipid or lipid–protein interactions were enhanced and may have resulted in the breakdown of larger domains through increasing lipid mixing or by stronger packing. The increase in cholesterol content could also promote the creation of new sites for domain nucleation, which would also result in the appearance of more domains of smaller size.

Alternatively, in vitro studies investigating domain morphology in a defined four system mixture of synthetic lipids have correlated line tension with domain size. In this system, increasing unsaturation in the L_d phase resulted in an increase in domain size from the nanoscopic to the macroscopic range [94]. While nanoscopic domain formation was not observed with microscopy, the presence of immiscible phases within the mixture was detected using neutron scattering [96]. Increase in domain size was suggested to be due to greater hydrophobic mismatch between the phases resulting in greater line tension at the phase interface. In order to overcome the negative energy cost [91], domains will coalesce, reducing the interfacial perimeter [94]. Thus, in terms of the data presented here, cholesterol depletion may have caused increased hydrophobic mismatch and the resulting increase in line tension then led to the formation of larger domains.

Changes in the shape of domains could be due to both increased lipid packing upon compression as well as higher localized cholesterol levels (Fig. 4D). Using a length to width ratio, with values closer to 1 equating to a roughly circular shape and values further from 1 indicating increasing elongation, the shape of the domains can be quantitatively compared. Higher proportions of cholesterol tended to result in an elongation of the domains. The trend is similar to that observed for domain size: the domains in the extracts from cholesterol loaded CV elongate at 15 mN/m then remain at a relatively constant shape; for the other treatments, the domains did not reach this level of elongation until much higher pressures. As mentioned before, the presence of circular domains indicated that the line tension between the immiscible phases within the monofilm was the dominant force. In contrast, other interactions, for example between molecular dipoles, would favor domain branching [97]. Thus, it is perhaps not surprising that with increasing compression, the change in line tension resulted in a distortion in the domain shape from circular to elongated. This has been previously attributed to shear force [92]. While we might speculate that cholesterol concentrations in native vesicle membranes are optimized to support fusion, more work is needed to better characterize the effects of cholesterol content on local membrane physical properties and thus fusion phenotypes.

5. Summary and conclusions

Comparison of thermodynamic properties between monolayers and bilayers indicate that the lateral pressure of native biomembranes is in the range of 30–35 mN/m [55]. At these high surface pressures, cholesterol composition has no effect on domain size in CV extracts. This would suggest that local cholesterol concentration in native membranes is sufficient to form 'completely' condensed domains. On the other hand, at >30 mN/m domain frequency and total domain area showed a strong dependence on cholesterol composition. Extracts from cholesterol depleted (~12 mol%), control (~16 mol%) and cholesterol loaded (~22 mol%) CV yielded ~200, ~300 and >400 domains, respectively; this amounted to ~2%, ~3% and >4% total domain area within the membrane, respectively. A decrease in cholesterol and number of domains correlated with a decrease in the Ca^{2+} sensitivity of triggered membrane fusion. Interestingly, an increase in vesicle membrane cholesterol above the native level, increased the formation of L_C domains above native conditions but was not associated with an increase in the Ca^{2+} sensitivity of fusion. Thus, a critical cholesterol concentration is necessary for normal lipid domain formation and optimal fusion efficiency, yet excess L_C membrane area alone is not functionally beneficial.

The depletion of cholesterol [12,13,27] and sphingomyelin [14] both result in a decrease in the extent and Ca^{2+} sensitivity of triggered fusion. This is presumably due to the lateral diffusion, loss of organization and/or poor interaction between proteins involved in docking, priming, Ca^{2+} sensing and triggering as a result of domain dispersal. It may also involve disruption of cholesterol acting directly as a co-factor for optimal membrane protein function. Another parallel possibility involves the loss of other critical lipids at the fusion site, including phosphatidylethanolamine, phosphatidylserine and polyphosphoinositides which have all been shown to have select roles in the FFM and PFM [27,34]. While cholesterol and sphingomyelin are critical, the precise composition and organization of lipid domains associated with the docking and fusion site remain speculative [9]. Indeed, while direct effects on functions such as fusion pore opening and expansion have been measured [98–100], the immediate cholesterol, protein, and lipid interactions that underlie these critical functions remain to be resolved in the detail necessary for a truly integrated understanding of the triggered release process (i.e. the functional molecular make-up and interactions that define the FFM and PFM).

Here we show that depletion of vesicle membrane cholesterol results in the formation of larger domains which hinder the process of fusion. While multiple models for putative domains relevant for vesicle fusion have been proposed [9], our findings would suggest that Ca^{2+} regulated membrane fusion is promoted in the presence of smaller domains; these could promote fusion as the point of contact between the membranes requires the presence of multiple lipids with high curvature, many of which favor existence in the more fluid L_d phase rather than the rigid L_o phase. Therefore while the necessary molecular machinery for the docking of the two membranes may well be contained within the domains, the presence of L_d phase surface area is required for the fusion event to take place. This is where modulation of fusion dynamics by cholesterol becomes important. Depletion of cholesterol results in increased line tension, causing a coalescence of domains [92]; these larger domains may disrupt the necessary temporal–spatial distribution of fusion machinery, and more importantly, limit the available adjacent L_d surface area required. Thus, alterations in fusion parameters following cholesterol depletion reflect a reduction in both the FFM as well as the PFM due to the dual role of the sterol. As cholesterol acts as a fusogenic lipid, the number of fusion machines is decreased. Moreover the efficiency is reduced as cholesterol is a key membrane organizer and lower levels result in a non-native distribution of necessary fusion components within the membrane.

It should be noted that the monolayers do not directly reflect native membrane dynamics as proteins are under-represented and effects of asymmetry are not assessed. Additionally, the domains seen may represent a coalescence of smaller native domains under our experimental conditions. Nonetheless, several important observations have been made: (i) lipid composition of CV membrane supports the formation of L_E domains within a L_C matrix; (ii) cholesterol depletion interferes with domain formation which correlates with a decrease in the Ca^{2+} sensitivity of triggered fusion; and (iii) supplementation with excess cholesterol enhances domain formation but has no measureable effect on the fusion mechanism. While these findings do not yet enable us to define the nature of the docking and fusion site, they support the likelihood of certain local structures, including the possibility of a contiguous cholesterol-enriched microdomain with regions of varied fluidity that could include the fusion site composed of select lipids [9]. Along with physiological and biochemical studies [12–14,39], these data thus

continue to support the hypothesis that lipid domains enriched in cholesterol and sphingomyelin localize and regulate the efficiency of docking and Ca^{2+} triggered membrane fusion. This does not exclude the possibility that the recruitment of other lipids and/or proteins (i.e. more fusion machines) may enhance fusion, but suggests that there are a limited number of PFM/FFM components available under native conditions [9,27,34,35]. Thus, cholesterol itself does not directly regulate Ca^{2+} sensitivity but instead acts as a membrane organizer (and possible co-factor) to ensure the optimal interaction of priming, docking, and fusion components of the triggered release machinery.

Transparency document

The Transparency document associated with this article can be found, in the online version.

Acknowledgements

J.R.C. acknowledges funding support from the Canadian Institutes of Health Research (CIHR), the Natural Sciences and Engineering Research Council of Canada (NSERC), the National Health and Medical Research Council (NHMRC, Australia) (APP106532) and the University of Western Sydney, School of Medicine. E.J.P. acknowledges funding support from a Discovery Grant provided by NSERC.

References

[1] K. Simons, E. Ikonen, Functional rafts in cell membranes, Nature 387 (1997) 569–572.
[2] A. Rietveld, K. Simons, The differential miscibility of lipids as the basis for the formation of functional membrane rafts, Biochim. Biophys. Acta Rev. Biomembr. 1376 (1998) 467–479.
[3] X. Xu, R. Bittman, G. Duportail, D. Heissler, C. Vilcheze, E. London, Effect of the structure of natural sterols and sphingolipids on the formation of ordered sphingolipid/sterol domains (rafts). Comparison of cholesterol to plant, fungal, and disease-associated sterols and comparison of sphingomyelin, cerebrosides, and ceramide, J. Biol. Chem. 276 (2001) 33540–33546.
[4] B. Ramstedt, J.P. Slotte, Sphingolipids and the formation of sterol-enriched ordered membrane domains, Biochim. Biophys. Acta 1758 (2006) 1945–1956.
[5] R.G. Anderson, K. Jacobson, A role for lipid shells in targeting proteins to caveolae, rafts, and other lipid domains, Science 296 (2002) 1821–1825.
[6] M. Edidin, The state of lipid rafts: from model membranes to cells, Annu. Rev. Biophys. Biomol. Struct. 32 (2003) 257–283.
[7] D.A. Brown, E. London, Functions of lipid rafts in biological membranes, Annu. Rev. Cell Dev. Biol. 14 (1998) 111–136.
[8] K. Simons, D. Toomre, Lipid rafts and signal transduction, Nat. Rev. Mol. Cell Biol. 1 (2000) 31–39.
[9] M.A. Churchward, J.R. Coorssen, Cholesterol, regulated exocytosis and the physiological fusion machine, Biom. J. 423 (2009) 1–14.
[10] S. Chasserot-Golaz, J. Coorssen, F. Meunier, N. Vitale, Lipid dynamics in exocytosis, Cell. Mol. Neurobiol. 30 (2010) 1335–1342.
[11] K. Simons, M.J. Gerl, Revitalizing membrane rafts: new tools and insights, Nat. Rev. Mol. Cell Biol. 11 (2010) 688–699.
[12] M.A. Churchward, T. Rogasevskaia, J. Höfgen, J. Bau, J.R. Coorssen, Cholesterol facilitates the native mechanism of $Ca2^{+}$-triggered membrane fusion, J. Cell Sci. 118 (2005) 4833–4848.
[13] M. Churchward, T. Rogasevskaia, D. Brandman, H. Khosravani, P. Nava, J. Atkinson, J. Coorssen, Specific lipids supply critical negative spontaneous curvature—an essential component of native $Ca2^{+}$-triggered membrane fusion, Biophys. J. 94 (2008) 3976–3986.
[14] T. Rogasevskaia, J.R. Coorssen, Sphingomyelin-enriched microdomains define the efficiency of native $Ca2^{+}$-triggered membrane fusion, J. Cell Sci. 119 (2006) 2688–2694.
[15] A. Linetti, A. Fratangeli, E. Taverna, P. Valnegri, M. Francolini, V. Cappello, M. Matteoli, M. Passafaro, P. Rosa, Cholesterol reduction impairs exocytosis of synaptic vesicles, J. Cell Sci. 123 (2010) 595–605.
[16] A.J. Smith, S. Sugita, M.P. Charlton, Cholesterol-dependent kinase activity regulates transmitter release from cerebellar synapses, J. Neurosci. 30 (2010) 6116–6121.
[17] T.V. Waseem, V.A. Kolos, L.P. Lapatsina, S.V. Fedorovich, Influence of cholesterol depletion in plasma membrane of rat brain synaptosomes on calcium-dependent and calcium-independent exocytosis, Neurosci. Lett. 405 (2006) 106–110.
[18] C.R. Wasser, M. Ertunc, X. Liu, E.T. Kavalali, Cholesterol-dependent balance between evoked and spontaneous synaptic vesicle recycling, J. Physiol. 579 (2007) 413–429.
[19] O. Zamir, M.P. Charlton, Cholesterol and synaptic transmitter release at crayfish neuromuscular junctions, J. Physiol. 571 (2006) 83–99.
[20] K.G. Ormerod, T.P. Rogasevskaia, J.R. Coorssen, A.J. Mercier, Cholesterol-independent effects of methyl-β-cyclodextrin on chemical synapses, PLoS One 7 (2012) e36395.
[21] B. Rituper, H.H. Chowdhury, J. Jorgacevski, J.R. Coorssen, M. Kreft, R. Zorec, Cholesterol-mediated membrane surface area dynamics in neuroendocrine cells, Biochim. Biophys. Acta 1831 (2012) 1228–1238.
[22] N. Wang, C. Kwan, X. Gong, E. de Chaves, A. Tse, F. Tse, Influence of cholesterol on catecholamine release from the fusion pore of large dense core chromaffin granules, J. Neurosci. Off. J. Soc. Neurosci. 30 (2010) 3904–3911.
[23] J. Zhang, R. Xue, W.-Y. Ong, P. Chen, Roles of cholesterol in vesicle fusion and motion, Biophys. J. 97 (2009) 1371–1380.
[24] J. Vikman, J. Jimenez-Feltström, P. Nyman, J. Thelin, L. Eliasson, Insulin secretion is highly sensitive to desorption of plasma membrane cholesterol, FASEB J. 23 (2009) 58–67.
[25] E.A. Cookson, I.L. Conte, J. Dempster, M.J. Hannah, T. Carter, Characterisation of Weibel–Palade body fusion by amperometry in endothelial cells reveals fusion pore dynamics and the effect of cholesterol on exocytosis, J. Cell Sci. 126 (2013) 5490–5499.
[26] M.A. Churchward, D.M. Brandman, T. Rogasevskaia, J.R. Coorssen, Copper (II) sulfate charring for high sensitivity on-plate fluorescent detection of lipids and sterols: quantitative analyses of the composition of functional secretory vesicles, J. Chem. Biol. 1 (2008) 79–87.
[27] T.P. Rogasevskaia, J.R. Coorssen, A new approach to the molecular analysis of docking, priming, and regulated membrane fusion, J. Chem. Biol. 4 (2011) 117–136.
[28] J. Zimmerberg, P. Blank, I. Kolosova, M.-S. Cho, M. Tahara, J. Coorssen, A stage-specific preparation to study the $Ca2^{+}$-triggered fusion steps of exocytosis: rationale and perspectives, Biochimie 82 (2000) 303–314.
[29] J.R. Coorssen, P.S. Blank, F. Albertorio, L. Bezrukov, I. Kolosova, P.S. Backlund Jr., J. Zimmerberg, Quantitative femto- to attomole immunodetection of regulated secretory vesicle proteins critical to exocytosis, Anal. Biochem. 307 (2002) 54–62.
[30] S.S. Vogel, K. Delaney, J. Zimmerberg, The sea urchin cortical reaction, Ann. N. Y. Acad. Sci. 635 (1991) 35–44.
[31] J.R. Coorssen, P.S. Blank, F. Albertorio, L. Bezrukov, I. Kolosova, X. Chen, P.S. Backlund, J. Zimmerberg, Regulated secretion: SNARE density, vesicle fusion and calcium dependence, J. Cell Sci. 116 (2003) 2087–2097.
[32] J.A. Szule, S.E. Jarvis, J.E. Hibbert, J.D. Spafford, J.E. Braun, G.W. Zamponi, G.M. Wessel, J.R. Coorssen, Calcium-triggered membrane fusion proceeds independently of specific presynaptic proteins, J. Biol. Chem. 278 (2003) 24251–24254.
[33] J.A. Szule, J.R. Coorssen, Revisiting the role of SNAREs in exocytosis and membrane fusion, Biochim. Biophys. Acta Mol. Cell Res. 1641 (2003) 121–135.
[34] T.P. Rogasevskaia, M.A. Churchward, J.R. Coorssen, Anionic lipids in $Ca2^{+}$-triggered fusion, Cell Calcium 52 (2012) 259–269.
[35] P.S. Abbineni, J.E. Hibbert, J.R. Coorssen, Critical role of cortical vesicles in dissecting regulated exocytosis: overview of insights into fundamental molecular mechanisms, Biol. Bull. 224 (2013) 200–217.
[36] M. Awasthi-Kalia, P.P. Schnetkamp, J.P. Deans, Differential effects of filipin and methyl-β-cyclodextrin on B cell receptor signaling, Biochem. Biophys. Res. Commun. 287 (2001) 77–82.
[37] M.L. Fanani, S. Härtel, R.G. Oliveira, B. Maggio, Bidirectional control of sphingomyelinase activity and surface topography in lipid monolayers, Biophys. J. 83 (2002) 3416–3424.
[38] A.V. Samsonov, I. Mihalyov, F.S. Cohen, Characterization of cholesterol–sphingomyelin domains and their dynamics in bilayer membranes, Biophys. J. 81 (2001) 1486–1500.
[39] K.L. Furber, M.A. Churchward, T.P. Rogasevskaia, J.R. Coorssen, Identifying critical components of native Ca2 + -triggered membrane fusion, Ann. N. Y. Acad. Sci. 1152 (2009) 121–134.
[40] R. Simson, E.D. Sheets, K. Jacobson, Detection of temporary lateral confinement of membrane proteins using single-particle tracking analysis, Biophys. J. 69 (1995) 989–993.
[41] E.D. Sheets, G.M. Lee, R. Simson, K. Jacobson, Transient confinement of a glycosylphosphatidylinositol-anchored protein in the plasma membrane, Biochemistry 36 (1997) 12449–12458.
[42] R. Simson, B. Yang, S.E. Moore, P. Doherty, F.S. Walsh, K.A. Jacobson, Structural mosaicism on the submicron scale in the plasma membrane, Biophys. J. 74 (1998) 297–308.
[43] A. Pralle, P. Keller, E.-L. Florin, K. Simons, J. Hörber, Sphingolipid–cholesterol rafts diffuse as small entities in the plasma membrane of mammalian cells, J. Cell Biol. 148 (2000) 997–1008.
[44] C. Dietrich, B. Yang, T. Fujiwara, A. Kusumi, K. Jacobson, Relationship of lipid rafts to transient confinement zones detected by single particle tracking, Biophys. J. 82 (2002) 274–284.
[45] K. Gaus, E. Gratton, E.P. Kable, A.S. Jones, I. Gelissen, L. Kritharides, W. Jessup, Visualizing lipid structure and raft domains in living cells with two-photon microscopy, Proc. Natl. Acad. Sci. 100 (2003) 15554–15559.
[46] C. Eggeling, C. Ringemann, R. Medda, G. Schwarzmann, K. Sandhoff, S. Polyakova, V.N. Belov, B. Hein, C. von Middendorff, A. Schönle, S.W. Hell, Direct observation of the nanoscale dynamics of membrane lipids in a living cell, Nature 457 (2009) 1159–1162.
[47] D.M. Owen, A. Magenau, D. Williamson, K. Gaus, The lipid raft hypothesis revisited—new insights on raft composition and function from super-resolution fluorescence microscopy, Bioessays 34 (2012) 739–747.
[48] B. Maggio, G.A. Borioli, M. Del Boca, L. De Tullio, M.L. Fanani, R.G. Oliveira, C.M. Rosetti, N. Wilke, Composition-driven surface domain structuring mediated by sphingolipids and membrane-active proteins, Cell Biochem. Biophys. 50 (2008) 79–109.

[49] D. Hoenig, D. Moebius, Direct visualization of monolayers at the air–water interface by Brewster angle microscopy, J. Phys. Chem. 95 (1991) 4590–4592.
[50] S. Hénon, J. Meunier, Microscope at the Brewster angle: direct observation of first-order phase transitions in monolayers, Rev. Sci. Instrum. 62 (1991) 936.
[51] H. Brockman, Lipid monolayers: why use half a membrane to characterize protein-membrane interactions? Curr. Opin. Struct. Biol. 9 (1999) 438–443.
[52] R. Brown, H. Brockman, Using monomolecular films to characterize lipid lateral interactions, in: T. McIntosh (Ed.), Lipid Rafts, vol. 398, Humana Press, 2007, pp. 41–58.
[53] T. Groger, S. Nathoo, T. Ku, C. Sikora, R.J. Turner, E.J. Prenner, Real-time imaging of lipid domains and distinct coexisting membrane protein clusters, Chem. Phys. Lipids 165 (2012) 216–224.
[54] S. Nathoo, J.K. Litzenberger, D.C. Bay, R.J. Turner, E.J. Prenner, Visualizing a multidrug resistance protein, EmrE, with major bacterial lipids using Brewster angle microscopy, Chem. Phys. Lipids 167–168 (2013) 33–42.
[55] D. Marsh, Lateral pressure in membranes, Biochim. Biophys. Acta Rev. Biomembr. 1286 (1996) 183–223.
[56] P. Dynarowicz-Łątka, A. Dhanabalan, O.N. Oliveira Jr., Modern physicochemical research on Langmuir monolayers, Adv. Colloid Interf. Sci. 91 (2001) 221–293.
[57] O. Maier, V. Oberle, D. Hoekstra, Fluorescent lipid probes: some properties and applications (a review), Chem. Phys. Lipids 116 (2002) 3–18.
[58] E. Prenner, G. Honsek, D. Honig, D. Mobius, K. Lohner, Imaging of the domain organization in sphingomyelin and phosphatidylcholine monolayers, Chem. Phys. Lipids 145 (2007) 106–118.
[59] D.C. Bay, R.A. Budiman, M.-P. Nieh, R.J. Turner, Multimeric forms of the small multidrug resistance protein EmrE in anionic detergent, Biochim. Biophys. Acta Biomembr. 1798 (2010) 526–535.
[60] D.C. Bay, R.J. Turner, Spectroscopic analysis of small multidrug resistance protein EmrE in the presence of various quaternary cation compounds, Biochim. Biophys. Acta Biomembr. 1818 (2012) 1318–1331.
[61] A. Cruz, L. Vázquez, M. Vélez, J. Pérez-Gil, Effect of pulmonary surfactant protein SP-B on the micro- and nanostructure of phospholipid films, Biophys. J. 86 (2004) 308–320.
[62] B. Maggio, C. Rosetti, G. Borioli, M. Fanani, M. Del Boca, Protein-mediated surface structuring in biomembranes, Braz. J. Med. Biol. Res. 38 (2005) 1735–1748.
[63] E. Mileykovskaya, W. Dowhan, Visualization of phospholipid domains in *Escherichia coli* by using the cardiolipin-specific fluorescent dye 10-N-nonyl acridine orange, J. Bacteriol. 182 (2000) 1172–1175.
[64] R.M. Epand, R.F. Epand, Lipid domains in bacterial membranes and the action of antimicrobial agents, Biochim. Biophys. Acta 1788 (2009) 289–294.
[65] J.R. Coorssen, P.S. Blank, M. Tahara, J. Zimmerberg, Biochemical and functional studies of cortical vesicle fusion: the SNARE complex and Ca^{2+} sensitivity, J. Cell Biol. 143 (1998) 1845–1857.
[66] P.S. Abbineni, E.P. Wright, T.P. Rogasevskaia, M.C. Killingsworth, C.S. Malladi, J.R. Coorssen, The sea urchin egg and cortical vesicles as model systems to dissect the fast, CA^{2+}-triggered steps of regulated exocytosis, Exocytosis Methods, vol. 83, Humana Press, 2014. 221–241.
[67] P.S. Blank, M.-S. Cho, S.S. Vogel, D. Kaplan, A. Kang, J. Malley, J. Zimmerberg, Submaximal responses in calcium-triggered exocytosis are explained by differences in the calcium sensitivity of individual secretory vesicles, J. Gen. Physiol. 112 (1998) 559–567.
[68] E.G. Bligh, W.J. Dyer, A rapid method of total lipid extraction and purification, Can. J. Biochem. Physiol. 37 (1959) 911–917.
[69] T. Barona, R.D. Byrne, T.R. Pettitt, M.J. Wakelam, B. Larijani, D.L. Poccia, Diacylglycerol induces fusion of nuclear envelope membrane precursor vesicles, J. Biol. Chem. 280 (2005) 41171–41177.
[70] K. Birdi, Lipid–protein monolayers, Lipid and Biopolymer Monolayers at Liquid Interfaces, Springer, 1989. 209–227.
[71] M.T. Le, J.K. Litzenberger, E.J. Prenner, Biomimetic model membrane systems serve as increasingly valuable in vitro tools, Advances in Biomimetics, In Tech, Rijeka, HR, 2011. 251–276.
[72] P. Heinig, S. Wurlitzer, T.M. Fischer, Spreading dynamics of 2D dipolar Langmuir monolayer phases, Eur. Phys. J. E: Soft Matter 14 (2004) 293–298.
[73] V.M. Kaganer, H. Möhwald, P. Dutta, Structure and phase transitions in Langmuir monolayers, Rev. Mod. Phys. 71 (1999) 779–819.
[74] G.D. Fidelio, B. Maggio, F.A. Cumar, Interaction of soluble and membrane proteins with monolayers of glycosphingolipids, Biochem. J. 203 (1982) 717–725.
[75] V.D. Vacquier, The isolation of intact cortical granules from sea urchin eggs: calcium ions trigger granule discharge, Dev. Biol. 43 (1975) 62–74.
[76] S.S. Vogel, P.S. Blank, J. Zimmerberg, Poisson-distributed active fusion complexes underlie the control of the rate and extent of exocytosis by calcium, J. Cell Biol. 134 (1996) 329–338.
[77] B. Discher, K. Maloney, W. Schief Jr., D. Grainger, V. Vogel, S. Hall, Lateral phase separation in interfacial films of pulmonary surfactant, Biophys. J. 71 (1996) 2583–2590.
[78] K. Nag, M. Fritzen-Garcia, R. Devraj, A.K. Panda, Interfacial organizations of gel phospholipid and cholesterol in bovine lung surfactant films, Langmuir 23 (2007) 4421–4431.
[79] K. Winsel, D. Hönig, K. Lunkenheimer, K. Geggel, C. Witt, Quantitative Brewster angle microscopy of the surface film of human broncho-alveolar lavage fluid, Eur. Biophys. J. 32 (2003) 544–552.
[80] C. Rosetti, R. Oliveira, B. Maggio, The Folch–Lees proteolipid induces phase coexistence and transverse reorganization of lateral domains in myelin monolayers, Biochim. Biophys. Acta Biomembr. 1668 (2005) 75–86.
[81] S. Keller, W. Pitcher III, W. Huestis, H. McConnell, Red blood cell lipids form immiscible liquids, Phys. Rev. Lett. 81 (1998) 5019.
[82] A. Radhakrishnan, T.G. Anderson, H.M. McConnell, Condensed complexes, rafts, and the chemical activity of cholesterol in membranes, Proc. Natl. Acad. Sci. 97 (2000) 12422–12427.
[83] S.R. Shaikh, A.C. Dumaual, L.J. Jenski, W. Stillwell, Lipid phase separation in phospholipid bilayers and monolayers modeling the plasma membrane, Biochim. Biophys. Acta Biomembr. 1512 (2001) 317–328.
[84] H.M. McConnell, A. Radhakrishnan, Condensed complexes of cholesterol and phospholipids, Biochim. Biophys. Acta Biomembr. 1610 (2003) 159–173.
[85] S.L. Veatch, S.L. Keller, Separation of liquid phases in giant vesicles of ternary mixtures of phospholipids and cholesterol, Biophys. J. 85 (2003) 3074–3083.
[86] P. Dynarowicz-Łątka, K. Hąc-Wydro, Interactions between phosphatidylcholines and cholesterol in monolayers at the air/water interface, Colloids Surf. B: Biointerfaces 37 (2004) 21–25.
[87] B.L. Stottrup, D.S. Stevens, S.L. Keller, Miscibility of ternary mixtures of phospholipids and cholesterol in monolayers, and application to bilayer systems, Biophys. J. 88 (2005) 269–276.
[88] B.L. Stottrup, S.L. Keller, Phase behavior of lipid monolayers containing DPPC and cholesterol analogs, Biophys. J. 90 (2006) 3176–3183.
[89] V. Janout, S. Turkyilmaz, M. Wang, Y. Wang, Y. Manaka, S.L. Regen, An upside down view of cholesterol's condensing effect: does surface occupancy play a role? Langmuir 26 (2010) 5316–5318.
[90] J.R. Coorssen, R. Rand, Effects of cholesterol on the structural transitions induced by diacylglycerol in phosphatidylcholine and phosphatidylethanolamine bilayer systems, Biochem. Cell Biol. 68 (1990) 65–69.
[91] A.J. Garcia-Saez, S. Chiantia, P. Schwille, Effect of line tension on the lateral organization of lipid membranes, J. Biol. Chem. 282 (2007) 33537–33544.
[92] D.J. Benvegnu, H.M. McConnell, Line tension between liquid domains in lipid monolayers, J. Phys. Chem. 96 (1992) 6820–6824.
[93] H.M. McConnell, R. De Koker, Equilibrium thermodynamics of lipid monolayer domains, Langmuir 12 (1996) 4897–4904.
[94] S.L. Goh, J.J. Amazon, G.W. Feigenson, Toward a better raft model: modulated phases in the four-component bilayer, DSPC/DOPC/POPC/CHOL, Biophys. J. 104 (2013) 853–862.
[95] E. London, Insights into lipid raft structure and formation from experiments in model membranes, Curr. Opin. Struct. Biol. 12 (2002) 480–486.
[96] F.A. Heberle, M. Doktorova, S.L. Goh, R.F. Standaert, J. Katsaras, G.W. Feigenson, Hybrid and nonhybrid lipids exert common effects on membrane raft size and morphology, J. Am. Chem. Soc. 135 (2013) 14932–14935.
[97] Y. Hu, K. Meleson, J. Israelachvili, Thermodynamic equilibrium of domains in a two-component Langmuir monolayer, Biophys. J. 91 (2006) 444–453.
[98] S. Scepek, J.R. Coorssen, M. Lindau, Fusion pore expansion in horse eosinophils is modulated by Ca^{2+} and protein kinase C via distinct mechanisms, EMBO J. 17 (1998) 4340–4345.
[99] S. Barg, C.S. Olofsson, J. Schriever-Abeln, A. Wendt, S. Gebre-Medhin, E. Renström, P. Rorsman, Delay between fusion pore opening and peptide release from large dense-core vesicles in neuroendocrine cells, Neuron 33 (2002) 287–299.
[100] Y. Kozlovsky, L.V. Chernomordik, M.M. Kozlov, Lipid intermediates in membrane fusion: formation, structure, and decay of hemifusion diaphragm, Biophys. J. 83 (2002) 2634–2651.